Journal of Zhejiang University-SCIENCE B (Biomedicine & Biotechnology)
ISSN 1673-1581 (Print); ISSN 1862-1783 (Online)
www.jzus.zju.edu.cn; www.springerlink.com
E-mail: jzus@zju.edu.cn

Transcriptional and translational responses of rapeseed leaves to red and blue lights at the rosette stage*#

Sheng-xin CHANG[1], Chu PU[1], Rong-zhan GUAN[1], Min PU[2], Zhi-gang XU†‡[1]

[1]*College of Agriculture, Nanjing Agricultural University, Nanjing 210095, China*

[2]*Lumlux Corp., Suzhou 215143, China*

†E-mail: xuzhigang@njau.edu.cn

Received Aug. 15, 2017; Revision accepted Nov. 26, 2017; Crosschecked July 10, 2018

Abstract: Under different red (R):blue (B) photon flux ratios, the growth performance of rapeseed (*Brassica napus* L.) is significantly different. Rapeseed under high R ratios shows shade response, while under high B ratios it shows sun-type morphology. Rapeseed under monochromatic red or blue light is seriously stressed. Transcriptomic and proteomic methods were used to analyze the metabolic pathway change of rapeseed (cv. "Zhongshuang 11") leaves under different R:B photon flux ratios (including 100R:0B%, 75R:25B%, 25R:75B%, and 0R:100B%), based on digital gene expression (DGE) and two-dimensional gel electrophoresis (2-DE). For DGE analysis, 2054 differentially expressed transcripts ($|\log_2(\text{fold change})|\geq 1$, $q<0.005$) were detected among the treatments. High R ratios (100R:0B% and 75R:25B%) enhanced the expression of cellular structural components, mainly the cell wall and cell membrane. These components participated in plant epidermis development and anatomical structure morphogenesis. This might be related to the shade response induced by red light. High B ratios (25R:75B% and 0R:100B%) promoted the expression of chloroplast-related components, which might be involved in the formation of sun-type chloroplast induced by blue light. For 2-DE analysis, 37 protein spots showed more than a 2-fold difference in expression among the treatments. Monochromatic light (ML; 100R:0B% and 0R:100B%) stimulated accumulation of proteins associated with antioxidation, photosystem II (PSII), DNA and ribosome repairs, while compound light (CL; 75R:25B% and 25R:75B%) accelerated accumulation of proteins associated with carbohydrate, nucleic acid, amino acid, vitamin, and xanthophyll metabolisms. These findings can be useful in understanding the response mechanisms of rapeseed leaves to different R:B photon flux ratios.

Key words: *Brassica napus* L.; Light emitting diode (LED) light; Comparative transcriptome and proteome; Leaf morphogenesis; Stress response

https://doi.org/10.1631/jzus.B1700408 **CLC number:** Q786

1 Introduction

Red (R) and blue (B) lights are the essential light qualities for plant growth. The photosynthetic pigment chlorophyll in plant leaves mainly absorbs 430–450 nm blue light and 640–660 nm red light. The exciting lights of photoreceptors (phytochrome, cryptochrome, and phototropin) are also in the red and blue light bands. Under different R:B photon flux ratios, the growth and development of plants are significantly different. Hernández and Kubota (2016) found that the chlorophyll content per leaf area, net photosynthetic rate, and stomatal conductance of cucumber leaves increased with the R:B photon flux ratio change from 100R:0B% to 0R:100B%. Hogewoning et al. (2010) found that cucumber leaves under 100R:0B%

‡ Corresponding author

* Project supported by the National Key R&D Program of China (No. 2017YFB0403903)

Electronic supplementary materials: The online version of this article (https://doi.org/10.1631/jzus.B1700408) contains supplementary materials, which are available to authorized users

ORCID: Zhi-gang XU, https://orcid.org/0000-0003-1750-4857

displayed a dysfunctional photosynthetic operation, while the leaves under 0R:100B% had a low photosynthetic ability but also showed healthy photosynthesis. Chang et al. (2016) found that along with the R:B photon flux ratio change from 100R:0B% to 0R:100B%, the rapeseed leaves changed from wrinkled blades and down-rolled margins to flat blades and slightly up-rolled margins; the leaves under high R ratios were similar to the shade-type leaves, while the leaves under high B ratios were similar to the sun-type leaves; the rapeseed leaves under compound light (CL) showed normal growth vigor, whereas the leaves under monochromatic light (ML) showed a stress response.

The light signal transduction in plant is initiated by the perception of photoreceptors to the light. Red light activates phytochrome, inhibits the activity of E3 ubiquitin ligase-COP1/SPA, and selectively represses the transcription factors *HY5*, *HYH*, *LAF1*, and *HFR1* under diverse conditions, which further regulates plant photomorphogenesis (Li et al., 2011). Blue light stimulates two signal transduction pathways mediated by cryptochrome: one is similar to the phytochrome-mediated pathway, and the other induces the development of the flower bud through regulating the reaction between cryptochrome and *CIB1* or other transcription factors (Liu et al., 2011). Blue light also activates several phototropin leading signal transduction pathways to regulate stomatal opening, chloroplast movement, and the rapid inhibition of hypocotyl growth (Inoue et al., 2010).

Transcriptional and translational studies mainly involve detection downstream of light signal transduction. Ma et al. (2001) found that the transcriptional patterns of *Arabidopsis* seedlings under red, blue, and white lights were similar; compared with dark treatment, light signal promoted 26 cell pathways including photosynthesis and starch, sucrose and cell wall synthesis. Wang et al. (2013) found that the transcriptional patterns of kelp under blue and white light were similar, while under red light it was different. Kim et al. (2006) compared the proteomes of wild-type and phytochrome mutant *Arabidopsis* seedlings under red, far-red, and blue lights, and found that the differentially expressed proteins among them were mainly metabolic enzymes, such as ribulose 1,5-bisphophate carboxylase/oxygenase which was involved in Calvin cycle, and thioglucosidase which was involved in glucoside bond hydrolyzation. Yang et al. (2008) examined wild-type and cryptochrome mutant *Arabidopsis* seedlings under blue and white lights and in the dark, and found that the differentially expressed proteins were involved in energy transformation, metabolism pathways, stress response, and detoxification. As far as we know, the transcriptome and proteome of plants under different R:B photon flux ratios have not been detected before.

In the present study, the transcriptional and translational responses of rapeseed leaves to four different R:B photon flux ratios were investigated. The characterization of the differentially expressed genes and proteins increased our knowledge of the mechanisms of the morphogenesis divergence of rapeseed leaves grown under high R ratios and high B ratios, and the complex mechanisms of ML-induced stress.

2 Materials and methods

2.1 Plant materials and growth conditions

Brassica napus cv. "Zhongshuang 11" was grown in light emitting diode (LED)-growth chambers (Optrun Co., Nanjing, China) for three weeks, as described by Chang et al. (2016). The LED panels in the chambers are a mix of red LEDs (peak wavelength 635 nm, full width at half maximum 14 nm; Fig. S1a) and blue LEDs (peak wavelength 450 nm, full width at half maximum 16 nm; Fig. S1b). The ratios of the R:B photon flux, including 100R:0B%, 75R:25B%, 25R:75B%, and 0R:100B% at (550±20) μmol/(m^2·s), which are close to the mean photon flux in the rapeseed field in the lower reaches of the Yangtze river in mid-September, were modulated by adjusting the operating current of the red and blue LEDs. The photoperiod was 12 h/12 h day/night. The growth parameters were measured on at least five biological replicates. Three biological replicates of the top second leaves grown under each treatment were collected and immediately frozen in liquid nitrogen. The samples were then maintained at −80 °C until RNA and protein extraction.

2.2 RNA isolation and digital gene expression (DGE) library construction and sequencing

Total RNA from each leaf sample was extracted using RNA plant reagent kits (Tiangen Company, Beijing, China). The quality and integrity of the RNA

samples were checked using the NanoPhotometer spectrophotometer (IMPLEN, CA, USA) and the Bioanalyzer 2100 system (Agilent Technologies, CA, USA). The RNAs derived from three biological replicates of each treatment were combined to generate each complementary DNA (cDNA) library. The cDNA libraries were prepared using the NEBNext Ultra RNA Library Prep Kit (Illumina, NEB, USA) according to the manufacturer's recommendations. The final RNA-seq was performed on the HiSeq 2500 platform (Illumina, NEB, USA).

2.3 Bioinformatics analysis for RNA-seq data

Raw sequencing data were processed through the FASTX-Toolkit pipeline (http://hannonlab.cshl.edu/fastx_toolkit) and FastQC (http://www.bioinformatics.babraham.ac.uk/projects/fastqc) to remove the read adapters and low-quality reads, respectively.

In order to avoid the influence of the homologous genes between A_n (*Brassica rapa*) and C_n (*Brassica oleracea*) subgenomes of the rapeseed in DGE analysis, the A_n subgenome (Wang et al., 2011) was chosen as the reference genome, and the genome index was built using Bowtie (http://bowtie-bio.sourceforge.net/index.shtml). The single-end clean reads were aligned to the reference genome using TopHat (http://ccb.jhu.edu/software/tophat). HTSeq (http://htseq.readthedocs.io/en/release_0.10.0/tour.html) was used to count the read numbers mapped to each gene. EdgeR (http://www.bioconductor.org/packages/release/bioc/html/edgeR.html) was used to adjust the read counts through one scaling normalized factor, and reads per kilobase of exon model per million mapped reads (RPKM) were calculated at the same time.

DEGseq (http://www.bioconductor.org/packages/release/bioc/html/DEGseq.html) was used to analyze the differential expression of each of the two treatments. The *P* values were adjusted using the Benjamini and Hochberg method. $|\log_2(\text{fold change})| \geq 1$ and corrected $q<0.005$ were set as the threshold for significantly differential expression.

Blast2GO (http://www.blast2go.com) and KEGG Mapper (http://www.genome.jp/kegg/mapper.html) were used to annotate the differentially expressed genes. Gene ontology (GO) enrichment analysis was also implemented by Blast2GO. GO terms with *P*-value less than 0.05 were considered significantly enriched by differentially expressed genes.

2.4 qRT-PCR analysis

To confirm the RNA-seq results, quantitative reverse transcription-polymerase chain reaction (qRT-PCR) was conducted to check the expression of putative light-quality-responding genes using SYBR Green (TaKaRa Biotechnology Co., Ltd., Dalian, China) and performed on an ABI 7300 Real-Time PCR System (Applied Biosystems Foster City, CA, USA). The primers of the key genes of interest were designed using Primer Premier 5.0 (Premier Biosoft International, CA, USA) (Table S1). The *EF-1-α* gene was selected as an internal control (Qi et al., 2010). The reaction settings consisted of 4 min at 95 °C and 40 cycles of 15 s at 95 °C, 20 s at 60 °C, and 40 s at 72 °C. The qRT-PCR was repeated three times for each sample. The relative mRNA level was calculated using the $2^{-\Delta\Delta C_T}$ model embedded in Microsoft Excel.

2.5 Protein extraction and quantification

Protein extraction was performed according to the method described by Wang et al. (2006). Briefly, rapeseed leaves were homogenized in 10% trichloroacetic acid (TCA)/acetone (containing 0.07% dithiothreitol (DTT)) and then precipitated for 1.5 h at −20 °C, centrifuged at 1600*g* for 3 min at 4 °C and the supernatant was removed. The centrifugation steps were repeated in 80% methanol plus 0.1 mol/L ammonium acetate and in 80% acetone (0.07% DTT) in sequence. After air drying at room temperature for 10 min, the powder was incubated at 4–8 ml/g 1:1 phenol (pH 8.0)/sodium dodecyl sulfate (SDS) buffer for 5 min. It was centrifuged and the upper phenol phase was collected. Then methanol containing 0.1 mol/L ammonium acetate was added and stored at −20 °C overnight. This was centrifuged and the supernatant discarded. The pellet was washed in 100% methanol (0.07% DTT) and 80% acetone in sequence. After air drying at room temperature, the protein powder was resuspended in rehydration buffer (7 mol/L urea, 0.04 g/ml 3-[(3-cholamidopropyl) dimethyl ammonio]-1-propanesulfonate (CHAPS), 65 mmol/L DTT, 0.2% pH 4–7 ampholytes (Bio-Rad, CA, USA), 2 mol/L thiourea, and 0.01 g/L bromophenol blue). The protein concentration was determined according to the method described by Bradford (1976).

2.6 Two-dimensional gel electrophoresis (2-DE) and staining

Protein solution (containing 2.2 mg proteins) was applied to 17 cm ReadyStrip IPG Strips (Bio-Rad), and isoelectric focusing was performed on a PROTEAN isoelectric focusing system (Bio-Rad) for a total of 60 kV·h at 19 °C. After the first dimension, the strips were equilibrated twice and the second dimension was performed in SDS-polyacrylamide gel electrophoresis (PAGE) as the common process (Zhuang et al., 2013). The gels were then stained with colloidal Coomassie brilliant blue G-250 (1.2 g/L G-250, 0.1 g/ml phosphoric acid, 0.1 g/ml ammonium sulfate, and 20% methanol).

2.7 Image acquisition and data analysis

Gels were imaged using the Versa Doc Imaging System 4000MP (Bio-Rad), and the images were analyzed using PDQuest 8.0.1 software (Bio-Rad). Each treatment was evaluated separately and each biological sample was analyzed in triplicate. For normalization, the total density in gel image procedure was used, in which the raw quantity of each spot in a member gel is divided by the total intensity value of all the pixels in the image. An assumption of the model applied in this procedure is that the total density of an image is relatively consistent from gel to gel. Between-sample differences in normalized expression levels ≥2-fold were regarded as significant, and the significance of differences in expression levels was assessed using Student's *t*-tests, setting the significance threshold at $P<0.05$.

2.8 Mass spectrometric analysis and data processing

Selected protein spots were subjected to digestion with trypsin, matrix-assisted laser desorption/ionization mass spectrometry (MALDI-MS), and liquid chromatography-tandem mass spectrometry (LC-MS/MS) analysis, then the MS and MS/MS data were searched by MASCOT against the MSDB protein database. All above procedures were described by Zhuang et al. (2013).

3 Results

3.1 Growth of rapeseed seedlings under different R:B photon flux ratios

Under 100R:0B% treatment, the rapeseed seedlings showed loose plant type, while under B-containing treatments, the seedlings showed compact plant type (Fig. 1). The seedlings under 75R:25B% treatment were the tallest, those under 100R:0B% treatment were the shortest, and the heights of the seedlings under 25R:75B% and 0R:100B% treatments were median (Table 1). The root length and stem width of the seedlings showed a similar tendency to the plant height.

Under different R:B photon flux ratios, the development rate of the seedlings was consistent. After 21 d exposure, all seedlings reached eight leaves and a whorl stage. However, the leaf age of the seedlings grown under different light qualities was different. Except for 75R:25B% treatment, all the other treatments showed leaf presenility and abscission, the

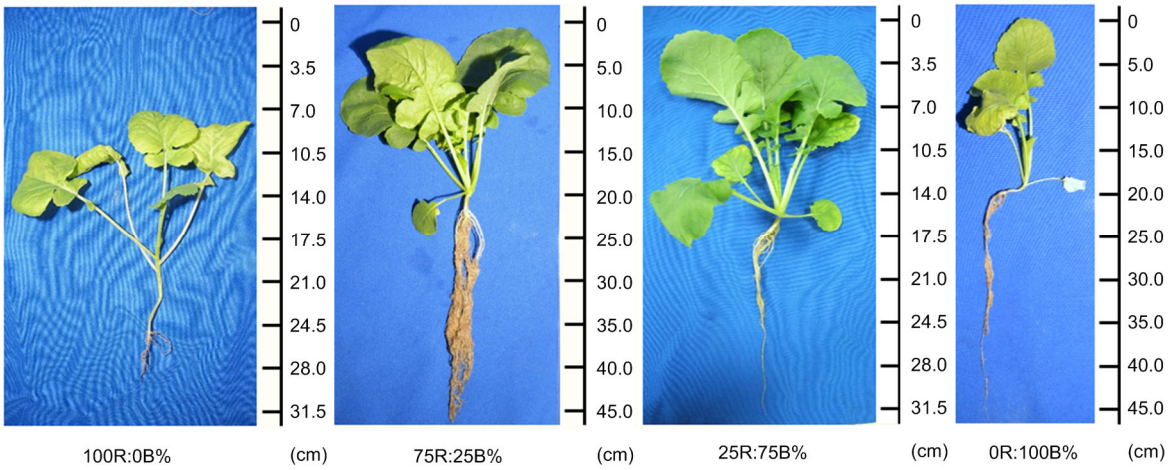

Fig. 1 Effects of different combinations of red (R) and blue (B) lights on the growth of rapeseed

25R:75B% treatment was left with 7.0 living leaves, and the 0R:100B% and 100R:0B% treatments had only 4.6 and 5.0 living leaves, respectively (Table 1). The fresh mass and dry mass of seedlings grown under 75R:25B% were the greatest, followed by 25R:75B%, 0R:100B%, and 100R:0B%.

3.2 DGE profiling of specific genes in response to different R:B photon flux ratios

To understand the effect of red and blue lights on the growth of rapeseed leaves, the regulation of gene expression was investigated using comparative DGE profiling analysis. After filtering dirty tags from the raw data, a total of 7037118–10391052 clean tags were obtained (NCBI SAR: SRP060320). Under $|\log_2(\text{fold change})|\geq 1$ and $q<0.005$ parameter control, DEGseq software identified the differentially expressed genes between each of the two treatments (File S1). The results showed that the numbers of differentially expressed genes between 100R:0B% and CL treatments were the greatest, and the numbers of up- or down-regulated genes in 100R:0B% treatment were all above 450 compared with CL treatments; the numbers of up- or down-regulated genes in 100R:0B% treatment were about 320 compared with 0R:100B% treatment; the numbers of up- or down-regulated genes in 0R:100B% were about 150 compared with CL; the numbers of differentially expressed genes between CLs were the least, with the numbers of up- or down-regulated genes at only about 110 (Table 2). In total, there were 2054 differentially expressed genes among the four treatments.

Using *K*-means and hierarchical methods, the treatments were clustered based on the RPKM of the differentially expressed genes. The result showed that the transcriptional patterns of 75R:25B% and 25R:75B% were the closest, followed by 0R:100B%, and 100R:0B% was the farthest (Fig. 2). This indicated that the B-induced transcriptional pattern holds the dominant position in the transcriptome of the CL.

Three hundred and twenty-three up-regulated genes and 320 down-regulated genes in 100R:0B% treatment compared with 0R:100B% treatment, and 107 up-regulated genes and 119 down-regulated genes in 75R:25B% compared with 25R:75B% were enriched using Blast2GO (Figs. S2 and S3). The results showed that the enriched GO terms in 100R:0B% and 75R:25B% treatments were all mainly cellular structural components, such as cell wall, cell membrane, plasmodesma, and vacuolar membrane. These components participated in plant epidermis development and anatomical structure morphogenesis. The GO terms enriched in 0R:100B% and 25R:75B% treatments were mainly chloroplast-related components, such as chloroplast thylakoid membrane, chloroplast envelope, and plastoglobule. These components joined in photosynthesis and the carbon metabolic process (Figs. S2 and S3).

Table 1 Effects of different light qualities on the growth of rapeseed seedlings

Light quality treatment	Plant height (cm)	Root length (cm)	Stem width (cm)	Leaf number (piece)	Fresh mass (g)	Dry mass (g)
100R:0B%	$13.6^{c,d}$	4.7^{c}	0.21^{c}	5.0^{c}	2.7^{c}	0.33^{c}
75R:25B%	15.8^{a}	28.2^{a}	0.53^{a}	8.0^{a}	23.2^{a}	2.51^{a}
25R:75B%	14.6^{b}	15.4^{b}	0.39^{b}	7.0^{b}	13.6^{b}	1.05^{b}
0R:100B%	$14.0^{b,c}$	19.1^{b}	0.24^{c}	4.6^{c}	3.0^{c}	0.39^{c}

Different letters behind the values indicate significant difference between different light treatments (Tukey's pairwise multicomparison test, $P\leq 0.05$). Data are the means of five plants

Table 2 Differentially expressed genes between different light quality treatments

Light quality treatment	Number of differentially expressed genes			
	100R:0B%	75R:25B%	25R:75B%	0R:100B%
100R:0B%		466	575	323
75R:25B%	675		107	188
25R:75B%	869	119		146
0R:100B%	320	160	186	

The upper triangle denotes the number of up-regulated genes for the treatment in the line compared with the treatment in the row, and the lower triangle denotes the number of down-regulated genes for the treatment in the line compared with the treatment in the row

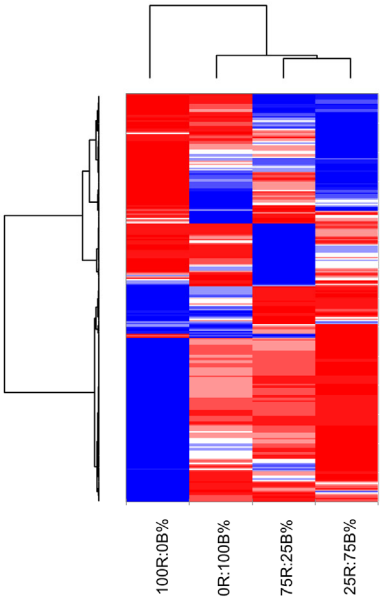

Fig. 2 Heatmap of cluster analysis for the different light quality treatments

Columns represent different samples, and rows represent differentially expressed genes. Red represents high expression, and blue represents low expression (Note: for interpretation of the references to color in this figure legend, the reader is referred to the web version of this article)

Venn diagram analysis identified a total of 279 up-regulated and 507 down-regulated genes in CL compared with 100R:0B% treatment (Figs. S4 and S5). The cellular component terms enriched in CL were mainly chloroplast, amyloplast, and Golgi membrane. The component participates in a wide range of biological processes, including energy metabolism, nitrogen metabolism, and secondary metabolism. The cellular component GO terms enriched in 100R:0B% were mainly cell wall, cell membrane, nucleus, and the subunits of ribosome. These components joined in the biological processes related to the morphogenesis process, stress response, and ribosome biogenesis. Venn analysis identified a total of 52 up-regulated and 38 down-regulated genes in CL compared with 0R:100B%. The GO terms enriched in CL were mainly the membrane part, endoplasmic reticulum, and cytosol, while the GO terms enriched in 0R:100B% were mainly the chloroplast component and chloroplast organization.

Ten genes were selected randomly and subjected to qRT-PCR confirmation (Fig. S6). *Bra004392* (expansin) and *Bra024415* (xyloglucan endotransglucosylase/hydrolase) showed higher expression levels in the high R ratio treatments. *Bra017201* (RNA-binding protein), *Bra014184* (cytochrome *c* biogenesis protein), *Bra005425* (LCHB1), and *Bra026426* (aldolase) showed higher expression levels in the high B ratio treatments. *Bra011408* (thioredoxin) and *Bra018611* (threonine aldolase) showed higher expression levels in CL, while *Bra013859* (acyl carrier protein) and *Bra002326* (chaperonin) showed higher expression levels in ML. The qRT-PCR expression patterns of these genes showed significant similarity to the RNA-seq data (r^2>0.82), which independently validated the gene expression analyses by RNA-seq.

3.3 2-DE analysis of rapeseed leaves under different R:B photon flux ratios

To explore the effect of red and blue lights on the growth of rapeseed leaves, a proteomic approach was applied. About 300 highly independent, outline clear and reproducible protein spots (Fig. 3) were consistently observed in all replicates after image analysis, with the molecular mass ranging from 14.4 to 116.0 kDa. From these, 37 differentially expressed spots (fold change≥2 and P<0.05) were identified for excision and analyzed using MALDI-tandem time-of-flight (TOF/TOF). Magnified views of some of the numbered protein spots showing differential expression are highlighted in Fig. 3. The numbers of the differentially expressed proteins between CL and ML were larger, while the numbers between 75R:25B% and 25R:75B%, and 100R:0B% and 0R:100B% were less (Table 3).

Table 3 Numbers of total and differentially expressed proteins from 2-DE maps for the rapeseed leaves grown under different light qualities

Light quality treatment	Spot number*	Number of differentially expressed proteins			
		100R:0B%	75R:25B%	25R:75B%	0R:100B%
100R:0B%	297±5				
75R:25B%	277±2	16			
25R:75B%	271±3	18	4		
0R:100B%	293±0	7	16	19	

* Data are expressed as mean±standard deviation (n=3)

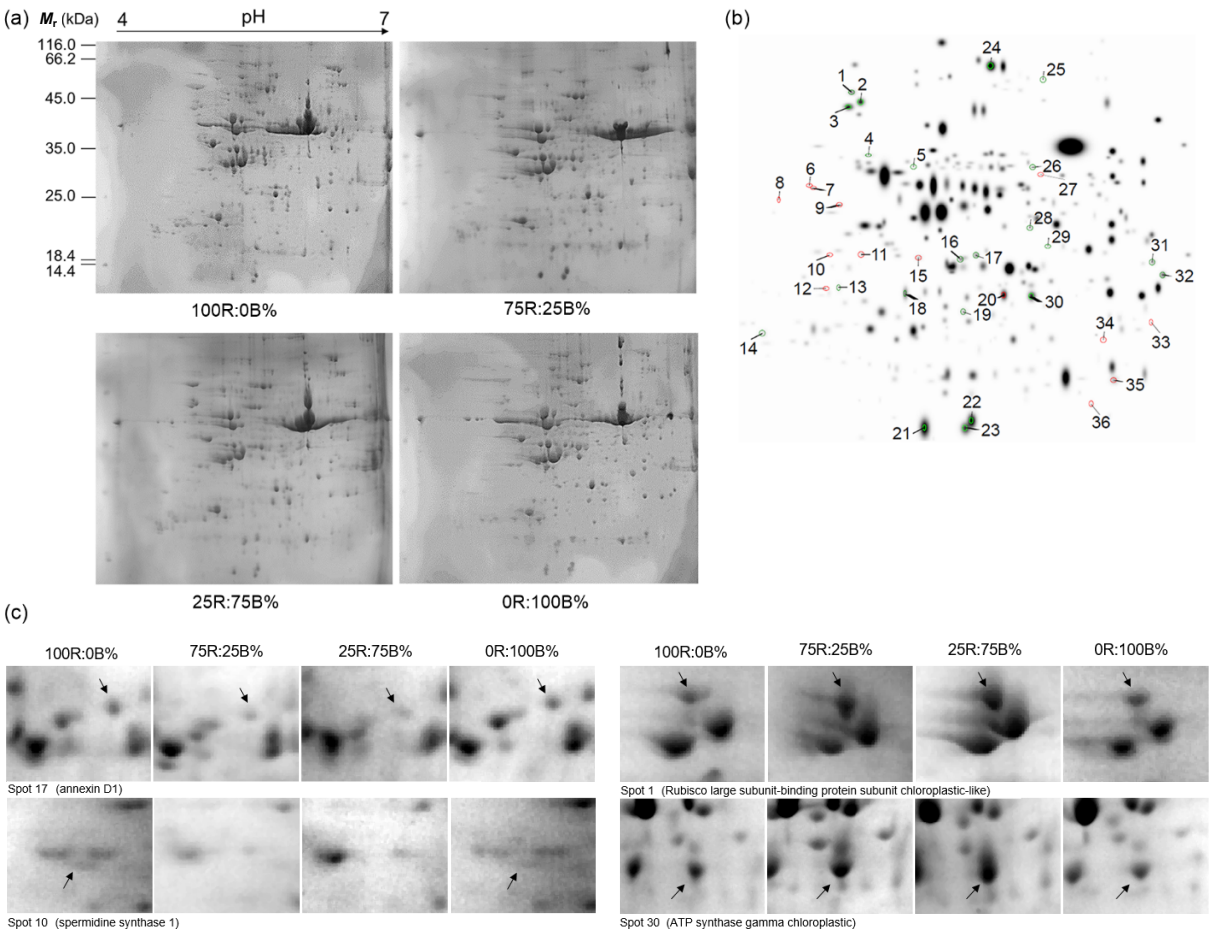

Fig. 3 2-DE gel profiles of total proteins from the different light quality treatments

(a) The 2-DE gels from four light quality treatments. M_r: relative molecular mass. (b) The master gel generated from PDQuest. The numbers of the 37 differentially expressed protein spots among the treatments were marked with arrows and numbers. The protein spot numbers correspond to the list in Table S2. Red circles in the master gel denote the proteins encoded by nuclear genome, and green circles denote the proteins encoded by chloroplast genome. (c) Magnified views of some of the differentially abundant proteins (Note: for interpretation of the references to color in this figure legend, the reader is referred to the web version of this article)

According to the metabolic and functional features described in GO annotation, Kyoto encyclopedia of genes and genomes (KEGG) pathways, and the literature concerning the identified proteins or their homologies (Table S2), the identified proteins could be classified into five categories as follows (Fig. 4a): stress and defense (32.4%), photosynthesis (32.4%), carbohydrate metabolism (8.8%), other metabolisms (14.7%), and unclassified (11.8%). Most of these proteins (62.2%) function in the chloroplast while the rest (37.8%) function in other cell parts. Through the function enrichment for the differentially expressed genes among the treatments, the stress and defense-related proteins were mainly enriched in ML compared with CL, while the light reaction of photosynthesis, CHO metabolism, and other metabolism-related proteins were mainly enriched in CL, and the dark reaction of the photosynthesis-related proteins showed irregular distribution.

4 Discussion

4.1 Correlation between transcriptome and proteome

DGE analysis mainly detected morphological-related genes between high R ratio treatments and high B ratio treatments, while only nine stress-related genes showed higher expression levels in 100R:0B%

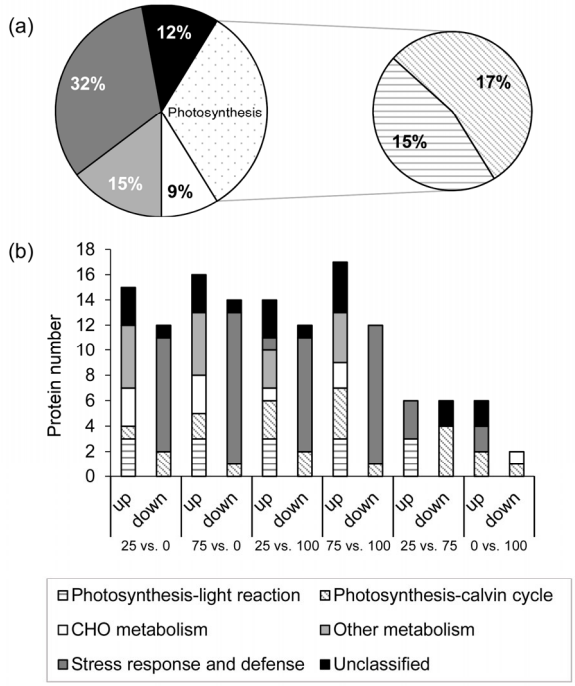

Fig. 4 Functional categories and the numbers of differentially expressed proteins in the rapeseed leaves grown under different light qualities

(a) The percentage of the differentially expressed functional categories. (b) The function enrichment of the differentially expressed proteins among different comparisons. 0, 25, 75, and 100 denote 100R:0B%, 75R:25B%, 25R:75B%, and 0R:100B%, respectively. CHO: carbohydrate

treatment compared with CL. In contrast, 2-DE mainly detected metabolism- and stress-related proteins between ML and CL, while only a "function unknown act domain-containing" protein showed higher expression in higher R ratio treatments compared with high B ratio treatments. The differentially expressed genes in DGE analysis did not overlap with the differentially expressed proteins in 2-DE analysis. This indicated that the correlation of transcriptome and proteome was low. Zhuang et al. (2013) found that the correlation coefficient between the differentially expressed proteins (2-DE) and genes (DGE) in the gibberellin 4 (GA_4)-treated Japanese apricot flower was only −0.28. Fan et al. (2011) found that the correlation coefficient of the overall proteome (isobaric tags for relative and absolute quantification (iTRAQ)) and transcriptome (DGE) data of sweet orange leaves infected by *Candidatus* Liberibacter was very low. Lan et al. (2012) studied phosphate-deficient *Arabidopsis* using the same method to roots, and obtained only a correlation coefficient of 0.51.

Transcriptome identifies the expression of RNAs, and this shows the short-term molecular change, while proteome identifies the accumulation of proteins, showing the long-term molecular change. This may be an important factor that explains the differences in transcriptome and proteome results. At the same time, the differences in analytical methods may also result in the discordance of transcriptome and proteome results. In the transcriptome analysis, in order to ensure data reliability, a strict q value (q<0.005) was used, and this might filter parts of differentially expressed genes. In the proteome analysis, the factors that may affect the protein detection include: (1) the phenol extraction method may cause partial loss of some proteins; (2) the pH of immobilized pH gradient (IPG) strips used in the study is 4.0–7.0, which causes some proteins to be too acid or bases not to be well separated; (3) because of the limit of database of the mass spectrometry, some proteins' specific function was not detected; (4) some proteins were excessively expressed and reached a saturation level in the 2-DE gels, or some proteins were slightly expressed and showed faint spots in the 2-DE gels, and then it was difficult to qualify the expression quantity.

4.2 Effect of red light on the expression of leaf morphogenesis-related genes

Under high R ratios, the leaf blade of rapeseed showed strong shade-type representation including loose plant type, wrinkled leaf blade, down-rolled leaf margin, and less-developed palisade tissue. This is in contrast to the sun-type leaves under high B ratios, with compact plant type, plate leaf blade, slightly up-rolled leaf margin, and well-developed palisade tissue (Fig. 1) (Chang et al., 2016). At the transcriptome level, through comparisons between 100R:0B% and 0R:100B%, and between 75R:25B% and 25R:75B%, GO analysis enriched a lot of morphogenesis-related terms in high R ratio treatments, such as cell wall, cell membrane, plant epidermis development, and anatomical structure morphogenesis. In the comparisons between 100R:0B% and CL, and between CL and 0R:100B%, similar results were also observed. Key genes in these terms were potentially related to the shade expression of rapeseed leaf (Fig. 5, Tables S3 and S4). The genes enriched in 100R:0B% compared with 0R:100B%, and in 75R:25B% compared with 25R:75B% were particularly analyzed.

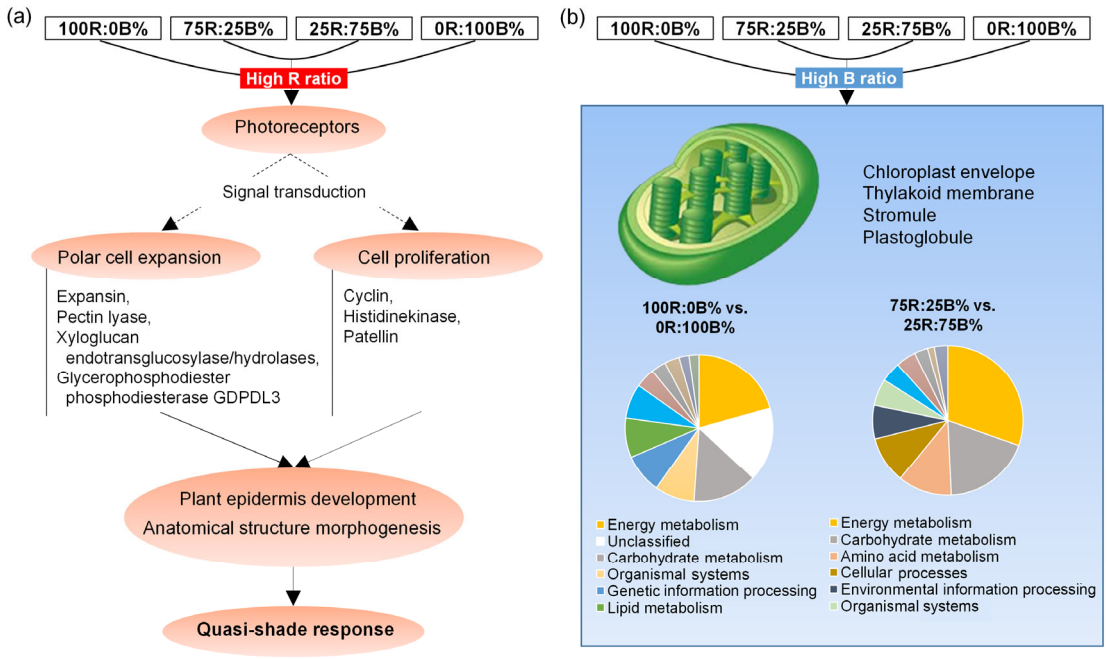

Fig. 5 Effects of light treatments with high R ratios (100R:0B% and 75R:25B%) and high B ratios (25R:75B% and 0R:100B%) on the growth of rapeseed leaves at the transcriptome level

(a) The downstream pathway of quasi-shade response in the rapeseed leaves induced by high R ratio lights, and the up-regulated GO terms and genes in 100R:0B% and 75R:25B% treatments. (b) The up-regulated GO terms in 25R:75B% and 0R:100B% treatments, and the result of GO level analysis for the "chloroplast" term in 0R:100B% and 25R:75B%. The first six differentially expressed terms were shown in the different-color chart legends (Note: for interpretation of the references to color in this figure legend, the reader is referred to the web version of this article)

Leaf morphology is very dependent on polar cell expansion (Tsukaya, 2006). According to Tsukaya (2002), cell polar expansion and development begins with cell wall loosening and is achieved by an increase in cell wall extensibility. Genes encoding expansin, pectate lyase, and xyloglucan endotransglucosylase/hydrolases, which participate in cell wall modification, were up-regulated in high R ratio treatments. Expansin facilitates cell wall stress relaxation and extension (Cosgrove, 2000); pectate lyase can degrade pectin and decrease cell wall integrity (Rose et al., 2004); xyloglucan endotransglucosylase/hydrolases can shear and connect the xylan. This has an important effect on the fiber connection of the cell wall. The expression of pectate lyase and xyloglucan endotransglucosylase/hydrolases is associated with the far-red- or green-induced petiole elongation of *Arabidopsis* (Roig-Villanova et al., 2006), while expansin may also function in the shade expression in high R ratio treatments. In the 100R:0B% treatment, glycerophosphodiester phosphodiesterase was also up-regulated compared with 0R:100B% treatment. This enzyme participates in the primary composition of the cell wall and plays an important role in the formation of cellulose crystals (Hayashi et al., 2008).

Cell proliferation is another essential mechanism for leaf morphogenesis, especially for the polar proliferation of epidemical cells. This can have a significant effect on leaf shape formation (Tsukaya, 2006; Tanaka et al., 2007). Compared with 0R:100B% treatment, 100R:0B% treatment enriched cyclin and histidine kinase. Cyclin can bind and regulate the cyclin-dependent kinase which is the main modulator for cell proliferation (Novikova et al., 2013). Histidine kinase is an important cytokinin receptor. It regulates the asymmetric division of vascular bundle cells and the formation of procambium (Hejátko et al., 2009). Compared with 25R:75B% treatment, 75R:25B% treatment enriched carrier protein—patellin, which joins in the formation of cell plate in the cell proliferation process (Peterman et al., 2004).

4.3 Effect of blue light on the expression of genes acting in chloroplasts

Blue light is beneficial for the formation of the sun-type chloroplast with lower and narrower grana thylakoid stacks. This is quite different from shade-type chloroplasts under red light that contain much higher and broader grana stacks (Buschmann et al., 1978; Lichtenthaler et al., 1980; Schuerger et al., 1997). At the transcriptome level, through comparisons between 100R:0B% and 0R:100B%, and between 75R:25B% and 25R:75B%, GO analysis enriched a lot of chloroplast-related terms in high B ratio treatments, such as chloroplast thylakoid membrane, chloroplast envelope, and plastoglobule. In the comparisons between 100R:0B% and CL, and between CL and 0R:100B%, similar results were also observed. Key genes in these terms were potentially related to the formation of the sun-type chloroplast of the rapeseed leaf (Fig. 5, Tables S5 and S6). The genes enriched in 100R:0B% compared with 0R:100B%, and in 75R:25B% compared with 25R:75B% were analyzed in particular.

The chloroplast-related terms contain chloroplast constitutive genes, mainly coding fibrillin and plastid-lipid-associated protein. These are involved in plastoglobule structural development and chromoplast pigment accumulation (Singh and McNellis, 2011). Many genes in chloroplast-related terms participate in energy metabolism, carbohydrate metabolism, genetic information processing, and so on (Fig. 5). The photosynthetic genes accounted for the largest proportion (24%–44%), of which photosystem II light-harvesting protein (PSII-LHCB) complex genes were the greatest number. Compared with 100R:0B% treatment, 0R:100B% treatment enriched 13 genes coding PSII-LHCB components, including *Lhcb1–4* and *Lhcb6–7*. Compared with 75R:25B% treatment, 25R:75B% treatment enriched 9 genes coding PSII-LHCB components, including *Lhcb1–3* and *psbY*. In both comparisons, all *ELIP1* was enriched. *LHCB* genes encode chlorophyll *a* and *b* binding proteins, which are the major antenna complex of PSII. *ELIP* genes encode early light-induced proteins, which are also chlorophyll-binding proteins and provide a photoprotective function. The expression levels of *LHCB* and *ELIP* are up-regulated when receiving more blue light in *Arabidopsis* and pea (Adamska et al., 1992; Anderson et al., 1999), while other studies have reported that plastoquinone (PQ) pool oxidization can increase the transcription of LHCB and PSII (Pfannschmidt, 2003). Recently, the associations of PQ pool oxidization with blue light exposure and PQ pool reduction with red light exposure were established (Jungandreas et al., 2014), suggesting that the redox state of the PQ pool may be the reason for the blue light-induced expression of PSII-LHCB, and the expression of *ELIP* may result from its functional relationship with LHCB. In our search for PSII photodamage under different spectra, B-biased damage was found (Chang et al., 2016). Whether the same B-biased expression of PSII-LHCB is related to this phenomenon is unknown, and more in-depth studies are required.

4.4 Effect of monochromatic lights on the expression of stress and defense-related proteins

The rapeseed seedlings grown under ML were obviously stressed, which showed the maximum quantum efficiency of PSII (F_v/F_m) of <8.0 and significantly fewer leaf numbers, lower fresh and dry mass than the seedlings grown under CL (Table 1) (Chang et al., 2016). At the proteomic level, ML treatments enriched a large number of stress response proteins, including antioxidant enzyme, antioxidant, and DNA and ribosome repair-related proteins (Fig. 6, Table S2). Reactive oxygen species (ROS) metabolisms are usually the initial reaction when abiotic or biotic stresses happen in the plants. At low concentrations, ROS act as signal molecules, while at high concentrations, ROS can injure the cell components (Pi et al., 2010). To defend against ROS damage, a plant will activate a series of protective mechanisms and the most important approach is to improve the activity of antioxidant enzymes. In the physiological study, the activity of catalase, superoxide dismutase, and peroxidase was promoted in the rapeseed leaves under ML (Chang et al., 2016). In the 2-DE analysis, annexin D1 (spots 16 and 17) was up-regulated 2.3–6.0 times in ML compared with CL. This protein does not have homology with the classical catalase, but the study in *Arabidopsis* found that this protein is very sensitive to H_2O_2 and will be enhanced in plants under heat, water, and salt stresses (Gorecka et al., 2005).

Glutathione is a standard antioxidant in plant cells. When the stress begins, the reduction level of glutathione increases (Tausz et al., 2004). Glutathione *S*-transferases (spots 35–37) are the key enzymes that

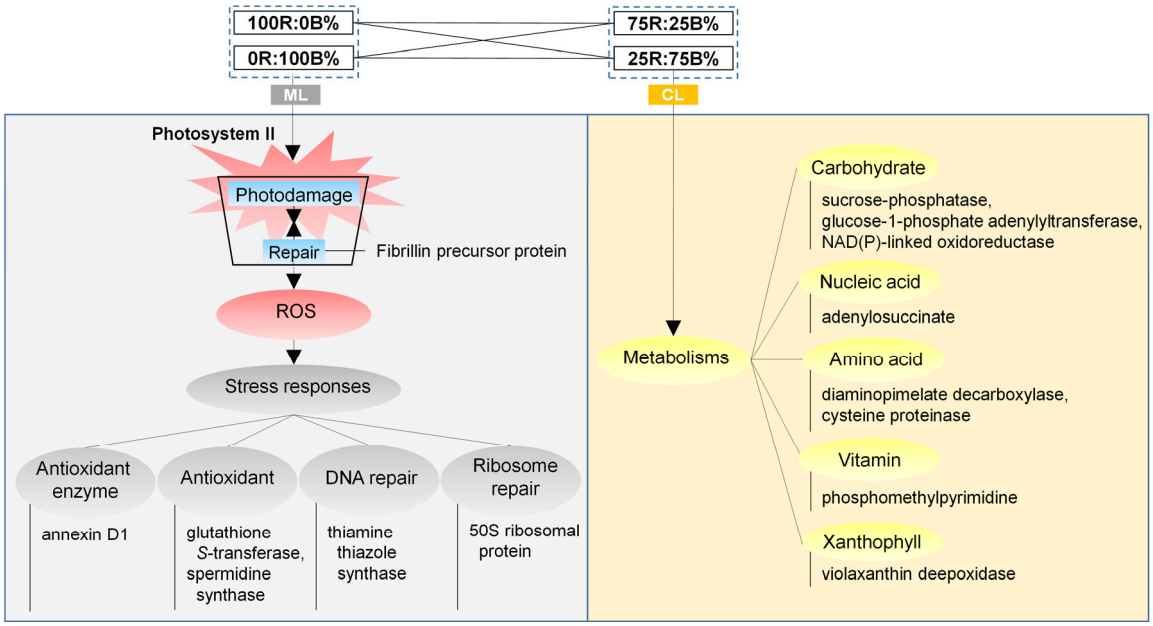

Fig. 6 Effects of monochromatic light (ML) and compound light (CL) on the growth of rapeseed leaves at the proteomic level

The left chart shows the pathway of ML-stress responses, and the right chart shows the metabolisms enhanced by CL

catalyze the initiation step of glutathione biosynthesis. Roxas et al. (2000) found that overexpression of glutathione *S*-transferases can improve the stress defense ability of transgenic tobacco. Spermidine plays an important role in regulating plant response under abiotic stress. It directly involves different metabolic pathways and hormonal interactions. Recent studies found that spermidine participates in the ROS signal transduction process, and when the plants suffer stress, the concentration of spermidine will increase (Liu et al., 2015). Spermidine synthase (spot 10) can synthesize putrescine to spermidine. Kasukabe et al. (2004) found that overexpression of spermidine synthase enhanced tolerance to multiple environmental stresses in transgenic *Arabidopsis*, and promoted the expression of various stress-regulated genes. In the present study, the amount of glutathione *S*-transferases was up-regulated to 6.2 times in ML compared with CL, while spermidine synthase showed detectable protein spots only in ML, and these indicated the important role of antioxidant in the ML stress responses.

The present study also identified thiamine thiazole synthases (spots 18 and 19), which can resist DNA destruction in ML. Machado et al. (1996) found that thiamine thiazole synthase is involved in the repair of DNA base excision, and can resist the damage from ultraviolet B (UVB). 50S ribosomal protein (spot 34), which is the component of 70S large subunit of chloroplast and mitochondrial ribosomes, was up-regulated in ML. Under UVB exposure, 50S ribosomal protein was also up-regulated, which can be considered as helping the cell resist damage caused by harmful radiation (Ulm and Nagy, 2005). Fibrillin precursor protein (spot 13) is regulated by abscisic acid response regulator and is involved in jasmonate biosynthesis during stress. Yang et al. (2006) found that this protein can enhance the tolerance of PSII toward light stress-triggered photoinhibition. Youssef et al. (2010) found that under high light combined with cold stress, the *Arabidopsis* plants with reduced levels of these proteins were impaired and their photosynthetic apparatus was inefficiently protected. Under ML, the up-regulated expression of fibrillin precursor protein corresponded with serious PSII damage (Chang et al., 2016). Carboxylesterase (spot 15) is involved in the biological degradation process of exogenous substances. In animals, carboxylesterase plays an important role in detoxification, while some evidence shows that this protein has an effect in a plant to resist pathogens (Marshall et al., 2003).

4.5 Effect of compound lights on the expression of metabolism-related proteins

CL promoted the expression of three kinds of photosynthetic proteins involved in the photoreaction stage of photosynthesis (Fig. 5, Table S2), including oxygen-evolving enhancer protein (OEE2), ATP synthase γ subunit, and ferredoxin-NADP. OEE2 (spots 21–23) was up-regulated two times as much in 75R:25B%, ATP synthase γ subunit (spot 30) was up-regulated 5.9–15.3 times in CL, and ferredoxin-NADP (spot 31) was up-regulated two times more in CL, compared with ML. These three kinds of photosynthetic proteins locate at different positions of the photosynthetic electron transport chain. OEE2 is the peripheral protein of the PSII-LHCB complex, and can protect the manganese complex from the attack of a reducing substance. The higher content of OEE2 in 75R:25B% may be related to the lower oxidation degree of PSII for the 75R:25B%-grown leaves. Compared with 75R:25B%, 25R:75B% has a higher proportion of blue light, which can result in the dissipation of PSII (Chang et al., 2016). At the same time, the PSII of the ML treatments suffered serious stress, but also withstood reduction pressure. Ferredoxin-NADP locates at an independent position in the photosynthetic electron transport chain, and is responsible for the electron transfer to NADP. ATP synthase γ subunit locates at the joint position of ATP synthase. Higher expression of these two kinds of proteins indicated higher NADPH and ATP synthesis ability, and these proteins may be related to the higher net photosynthetic rate in the CL-grown leaves (Chang et al., 2016).

Compared with photoreaction-related proteins, dark reaction-related proteins showed various expression patterns. Taking rubisco large subunit proteins (spots 1–3) as an example, the amount of spot 1 in CL was up-regulated 3.3–4.4 times compared with ML; the amount of spots 2 and 3 in 100R:0B% treatment was up-regulated two times compared with 75R:25B%; the amount of spots 2 and 3 in 75R:25B% and 0R:100B%, and in 100R:0B% and 25R:75B% was similar, respectively. The amount of transketolase (spot 24) in CL was up-regulated 2.5 times compared with ML; fructose-bisphosphate aldolase (spot 32) in CL was down-regulated 2.5–4.0 times compared with ML; ribulose bisphosphate carboxylase small subunit (spot 33) was up-regulated 4.0–8.4 times in high B ratio treatments compared with high R ratio treatments. The dark reaction proteins not only participate in photosynthesis, but also in other metabolisms, such as glycolysis, glyoxylate, and dicarboxylate metabolisms. The expression levels of these proteins are a comprehensive embodiment of all related metabolisms, and therefore show a relatively low association with the net photosynthetic rate compared with photoreaction-related proteins.

The present study identified three carbohydrate metabolism-related proteins in CL, including sucrose phosphatase (spot 28), glucose-1-phosphate adenylyltransferase (spot 5), and NAD(P)-linked oxidoreductase (spot 29). Sucrose phosphatase catalyzes the final step in sucrose synthesis, adenylyltransferase plays a key role in starch synthesis, and NAD(P)-linked oxidoreductase is involved in the secondary carbohydrate metabolism. The higher expression of these proteins may be related to the higher content of sucrose and starch in CL (Chang et al., 2016). Except carbohydrate metabolism, nucleic acid, amino acid, vitamin, and secondary metabolism-related proteins also showed higher expression levels in CL-grown leaves (Table S2, Fig. 6). Diaminopimelate decarboxylase (spot 26) participates in the biosynthesis of lysine, cysteine proteinase (spot 8) is involved in the decomposition of amino acids, adenylosuccinate synthetase (spot 27) is involved in the first step of adenine nucleotide biosynthesis, phosphomethylpyrimidine (spot 25) is involved in thiamine synthesis, and violaxanthin deepoxidase (spot 4) participates in the lutein cycle, which plays an important role in the carotenoid metabolism.

5 Conclusions

Under different R:B photon flux ratios, the transcriptome and proteome showed systemic change. Higher R ratio treatments induced the expression of epidermis development and anatomical structure morphogenesis-related genes, which may be related to the shade response of rapeseed leaves. Higher B ratio treatments induced the expression of chloroplast-related genes, which may be related to the formation of the sun-type chloroplast. ML induced the expression of stress response-related proteins, while CL promoted the expression of carbon and nitrogen metabolisms and secondary metabolism-related proteins.

Compliance with ethics guidelines

Sheng-xin CHANG, Chu PU, Rong-zhan GUAN, Min PU, and Zhi-gang XU declare that they have no conflict of interest.

This article does not contain any studies with human or animal subjects performed by any of the authors.

References

Adamska I, Ohad I, Kloppstech K, 1992. Synthesis of the early light-inducible protein is controlled by blue light and related to light stress. *Proc Natl Acad Sci USA*, 89(7): 2610-2613. https://doi.org/10.1073/pnas.89.7.2610

Anderson MB, Folta K, Warpeha KM, et al., 1999. Blue light-directed destabilization of the pea *Lhcb1*4* transcript depends on sequences within the 5' untranslated region. *Plant Cell*, 11(8):1579-1589. https://doi.org/10.1105/tpc.11.8.1579

Bradford MM, 1976. A rapid and sensitive method for the quantitation of microgram quantities of protein utilizing the principle of protein-dye binding. *Anal Biochem*, 72(1-2): 248-254. https://doi.org/10.1016/0003-2697(76)90527-3

Buschmann C, Meier D, Kleudgen HK, et al., 1978. Regulation of chloroplast development by red and blue light. *Photochem Photobiol*, 27(2):195-198. https://doi.org/10.1111/j.1751-1097.1978.tb07587.x

Chang SX, Li CX, Yao XY, et al., 2016. Morphological, photosynthetic, and physiological responses of rapeseed leaf to different combinations of red and blue lights at the rosette stage. *Front Plant Sci*, 7:1144. https://doi.org/10.3389/fpls.2016.01144

Cosgrove DJ, 2000. Loosening of plant cell walls by expansins. *Nature*, 407(6802):321-326. https://doi.org/10.1038/35030000

Fan J, Chen CX, Yu QB, et al., 2011. Comparative iTRAQ proteome and transcriptome analyses of sweet orange infected by "*Candidatus* Liberibacter asiaticus". *Physiol Plantarum*, 143(3):235-245. https://doi.org/10.1111/j.1399-3054.2011.01502.x

Gorecka KM, Konopka-Postupolska D, Hennig J, et al., 2005. Peroxidase activity of annexin 1 from *Arabidopsis thaliana*. *Biochem Biophys Res Commun*, 336(3):868-875. https://doi.org/10.1016/j.bbrc.2005.08.181

Hayashi S, Ishii T, Matsunaga T, et al., 2008. The glycerophosphoryl diester phosphodiesterase-like proteins SHV3 and its homologs play important roles in cell wall organization. *Plant Cell Physiol*, 49(10):1522-1535. https://doi.org/10.1093/pcp/pcn120

Hejátko J, Ryu H, Kim GT, et al., 2009. The histidine kinases CYTOKININ-INDEPENDENT1 and ARABIDOPSIS HISTIDINE KINASE2 and 3 regulate vascular tissue development in *Arabidopsis* shoots. *Plant Cell*, 21(7): 2008-2021. https://doi.org/10.1105/tpc.109.066696

Hernández R, Kubota C, 2016. Physiological responses of cucumber seedlings under different blue and red photon flux ratios using LEDs. *Environ Exp Bot*, 121:66-74. https://doi.org/10.1016/j.envexpbot.2015.04.001

Hogewoning SW, Trouwborst G, Maljaars H, et al., 2010. Blue light dose-responses of leaf photosynthesis, morphology, and chemical composition of *Cucumis sativus* grown under different combinations of red and blue light. *J Exp Bot*, 61(11):3107-3117. https://doi.org/10.1093/jxb/erq132

Inoue SI, Takemiya A, Shimazaki KI, 2010. Phototropin signaling and stomatal opening as a model case. *Curr Opin Plant Biol*, 13(5):587-593. https://doi.org/10.1016/j.pbi.2010.09.002

Jungandreas A, Schellenberger Costa B, Jakob T, et al., 2014. The acclimation of *Phaeodactylum tricornutum* to blue and red light does not influence the photosynthetic light reaction but strongly disturbs the carbon allocation pattern. *PLoS ONE*, 9(8):e99727. https://doi.org/10.1371/journal.pone.0099727

Kasukabe Y, He LX, Nada K, et al., 2004. Overexpression of spermidine synthase enhances tolerance to multiple environmental stresses and up-regulates the expression of various stress-regulated genes in transgenic *Arabidopsis thaliana*. *Plant Cell Physiol*, 45(6):712-722. https://doi.org/10.1093/pcp/pch083

Kim DS, Cho DS, Park WM, et al., 2006. Proteomic pattern-based analyses of light responses in *Arabidopsis thaliana* wild-type and photoreceptor mutants. *Proteomics*, 6(10): 3040-3049. https://doi.org/10.1002/pmic.200500670

Lan P, Li WF, Schmidt W, 2012. Complementary proteome and transcriptome profiling in phosphate-deficient Arabidopsis roots reveals multiple levels of gene regulation. *Mol Cell Proteomics*, 11(11):1156-1166. https://doi.org/10.1074/mcp.M112.020461

Li JG, Li G, Wang HY, et al., 2011. Phytochrome signaling mechanisms. *Arabidopsis Book*, 9:e0148. https://doi.org/10.1199/tab.0148

Lichtenthaler HK, Buschmann C, Rahmsdorf U, 1980. The importance of blue light for the development of sun-type chloroplasts. In: Senger H (Ed.), The Blue Light Syndrome. Springer, Berlin, Heidelberg, p.485-494. https://doi.org/10.1007/978-3-642-67648-2_45

Liu HT, Liu B, Zhao CX, et al., 2011. The action mechanisms of plant cryptochromes. *Trends Plant Sci*, 16(12):684-691. https://doi.org/10.1016/j.tplants.2011.09.002

Liu JH, Wang W, Wu H, et al., 2015. Polyamines function in stress tolerance: from synthesis to regulation. *Front Plant Sci*, 6(827):827. https://doi.org/10.3389/fpls.2015.00827

Ma LG, Li JM, Qu LJ, et al., 2001. Light control of Arabidopsis development entails coordinated regulation of genome expression and cellular pathways. *Plant Cell*, 13(12):2589-2607. https://doi.org/10.1105/tpc.010229

Machado CR, Costa de Oliveira RL, Boiteux S, et al., 1996. *Thi1*, a thiamine biosynthetic gene in *Arabidopsis thaliana*,

complements bacterial defects in DNA repair. *Plant Mol Biol*, 31(3):585-593. https://doi.org/10.1007/BF00042231

Marshall SDG, Putterill JJ, Plummer KM, et al., 2003. The carboxylesterase gene family from *Arabidopsis thaliana*. *J Mol Evol*, 57(5):487-500. https://doi.org/10.1007/s00239-003-2492-8

Novikova GV, Nosov AV, Stepanchenko NS, et al., 2013. Plant cell proliferation and its regulators. *Russ J Plant Physiol*, 60(4):500-506. https://doi.org/10.1134/S1021443713040109

Peterman TK, Ohol YM, McReynolds LJ, et al., 2004. Patellin1, a novel Sec14-like protein, localizes to the cell plate and binds phosphoinositides. *Plant Physiol*, 136(2):3080-3094. https://doi.org/10.1104/pp.104.045369

Pfannschmidt T, 2003. Chloroplast redox signals: how photosynthesis controls its own genes. *Trends Plant Sci*, 8(1): 33-41. https://doi.org/10.1016/S1360-1385(02)00005-5

Pi JB, Zhang Q, Fu JQ, et al., 2010. ROS signaling, oxidative stress and Nrf2 in pancreatic beta-cell function. *Toxicol Appl Pharm*, 244(1):77-83. https://doi.org/10.1016/j.taap.2009.05.025

Qi JN, Yu SC, Zhang FL, et al., 2010. Reference gene selection for real-time quantitative polymerase chain reaction of mRNA transcript levels in Chinese cabbage (*Brassica rapa* L. ssp. *pekinensis*). *Plant Mol Biol Rep*, 28(4):597-604. https://doi.org/10.1007/s11105-010-0185-1

Roig-Villanova I, Bou J, Sorin C, et al., 2006. Identification of primary target genes of phytochrome signaling. Early transcriptional control during shade avoidance responses in Arabidopsis. *Plant Physiol*, 141(1):85-96. https://doi.org/10.1104/pp.105.076331

Rose JK, Saladié M, Catalá C, 2004. The plot thickens: new perspectives of primary cell wall modification. *Curr Opin Plant Biol*, 7(3):296-301. https://doi.org/10.1016/j.pbi.2004.03.013

Roxas VP, Lodhi SA, Garrett DK, et al., 2000. Stress tolerance in transgenic tobacco seedlings that overexpress glutathione *S*-transferase/glutathione peroxidase. *Plant Cell Physiol*, 41(11):1229-1234. https://doi.org/10.1093/pcp/pcd051

Schuerger AC, Brown CS, Stryjewski EC, 1997. Anatomical features of pepper plants (*Capsicum annuum* L.) grown under red light-emitting diodes supplemented with blue or far-red light. *Ann Bot*, 79(3):273-282. https://doi.org/10.1006/anbo.1996.0341

Singh DK, McNellis TW, 2011. Fibrillin protein function: the tip of the iceberg? *Trends Plant Sci*, 16(8):432-441. https://doi.org/10.1016/j.tplants.2011.03.014

Tanaka H, Watanabe M, Sasabe M, et al., 2007. Novel receptor-like kinase ALE2 controls shoot development by specifying epidermis in *Arabidopsis*. *Development*, 134(9): 1643-1652. https://doi.org/10.1242/dev.003533

Tausz M, Šircelj H, Grill D, 2004. The glutathione system as a stress marker in plant ecophysiology: is a stress-response concept valid? *J Exp Bot*, 55(404):1955-1962. https://doi.org/10.1093/jxb/erh194

Tsukaya H, 2002. Leaf development. *Arabidopsis Book*, 1:e0072. https://doi.org/10.1199/tab.0072

Tsukaya H, 2006. Mechanism of leaf-shape determination. *Ann Rev Plant Biol*, 57:477-496. https://doi.org/10.1146/annurev.arplant.57.032905.105320

Ulm R, Nagy F, 2005. Signalling and gene regulation in response to ultraviolet light. *Curr Opin Plant Biol*, 8(5): 477-482. https://doi.org/10.1016/j.pbi.2005.07.004

Wang W, Vignani R, Scali M, et al., 2006. A universal and rapid protocol for protein extraction from recalcitrant plant tissues for proteomic analysis. *Electrophoresis*, 27(13):2782-2786. https://doi.org/10.1002/elps.200500722

Wang WJ, Wang FJ, Sun XT, et al., 2013. Comparison of transcriptome under red and blue light culture of *Saccharina japonica* (Phaeophyceae). *Planta*, 237(4):1123-1133. https://doi.org/10.1007/s00425-012-1831-7

Wang XW, Wang HZ, Wang J, et al., 2011. The genome of the mesopolyploid crop species *Brassica rapa*. *Nat Genet*, 43(10):1035-1039. https://doi.org/10.1038/ng.919

Yang Y, Sulpice R, Himmelbach A, et al., 2006. Fibrillin expression is regulated by abscisic acid response regulators and is involved in abscisic acid-mediated photoprotection. *Proc Natl Acad Sci USA*, 103(15):6061-6066. https://doi.org/10.1073/pnas.0501720103

Yang YJ, Li Y, Li X, et al., 2008. Comparative proteomics analysis of light responses in cryptochrome1–304 and Columbia wild-type 4 of *Arabidopsis thaliana*. *Acta Biochim Biophys Sin*, 40(1):27-37. https://doi.org/10.1111/j.1745-7270.2008.00367.x

Youssef A, Laizet Y, Block MA, et al., 2010. Plant lipid-associated fibrillin proteins condition jasmonate production under photosynthetic stress. *Plant J*, 61(3):436-445. https://doi.org/10.1111/j.1365-313X.2009.04067.x

Zhuang WB, Gao ZH, Wang LJ, et al., 2013. Comparative proteomic and transcriptomic approaches to address the active role of GA_4 in Japanese apricot flower bud dormancy release. *J Exp Bot*, 64(16):4953-4966. https://doi.org/10.1093/jxb/ert284

List of electronic supplementary materials

Fig. S1 Major technique parameters of different light spectral energy distributions under LED

Fig. S2 GO enrichment analysis of differentially expressed genes between 100R:0B% and 0R:100B%

Fig. S3 GO enrichment analysis of differentially expressed genes between 75R:25B% and 25R:75B%

Fig. S4 Venn analysis and GO enrichment analysis of differentially expressed genes between CL (75R:25B% and 25R:75B%) and 100R:0B%

Fig. S5 Venn analysis and GO enrichment analysis of differentially expressed genes between CL (75R:25B% and 25R:75B%) and 0R:100B%

Fig. S6 qRT-PCR analysis of ten random genes for the four light quality treatments

Table S1 Primers of ten randomly selected differentially expressed genes

Table S2 Thirty-seven proteins identified by MALDI-TOF/TOF MS in the rapeseed leaves grown under different light qualities

Table S3 Genes in photomorphogenesis-related GO terms enriched between 100R:0B% and 0R:100B%

Table S4 Genes in photomorphogenesis-related GO terms enriched between 75R:25B% and 25R:75B%

Table S5 Genes in chloroplast-related GO terms enriched between 100R:0B% and 0R:100B%

Table S6 Genes in chloroplast-related GO terms enriched between 75R:25B% and 25R:75B%

File S1 Differentially expressed genes between each of two light quality treatments identified by DEGseq

中文概要

题　目：红蓝光质下苗期油菜基因和蛋白表达特性的研究

目　的：研究不同比例红蓝光下苗期油菜表型、转录和蛋白水平的差异。

创新点：利用转录组和蛋白组技术对不同红蓝光质下油菜叶片的分子表达进行检测，并探讨了其与叶片表型响应的关系。

方　法：采用数字基因表达谱和双向电泳技术检测红蓝光处理后油菜叶片的基因和蛋白表达水平，并分析处理间的差异。

结　论：不同比例红蓝光下，油菜叶片转录组和蛋白组呈系统性变化。高比例红光诱发叶片表皮发育和解剖结构形态建成相关基因的表达，它们可能与高比红光诱发的遮阴应答相关。高比蓝光促进叶绿体相关基因的表达，它们可能与高比蓝光下阳生型叶绿体的形成相关。红蓝单色光诱发胁迫应答相关蛋白的表达，而红蓝复合光促进碳氮代谢和次生代谢相关蛋白的表达。

关键词：油菜；发光二极管光源；转录组和蛋白组；叶片表型；胁迫应答